Biochimica et Biophysica Acta, 691 (1982) 1–12
Elsevier Biomedical Press

BBA 71329

ALKALINE EARTH CATION BINDING TO LARGE AND SMALL BILAYER PHOSPHATIDYLSERINE VESICLES

A CALORIMETRIC AND POTENTIOMETRIC STUDY *

SELWYN J. REHFELD, LEE D. HANSEN, EDWIN A. LEWIS and DELBERT J. EATOUGH

Thermochemical Institute and Department of Chemistry, Brigham Young University, Provo, UT 84602 (U.S.A.)

(Received March 11th, 1982)

Key words: Calorimetry; Potentiometry; Alkaline earth; Phosphatidylserine vesicle; Ion binding

A study is reported of the interaction of alkaline earth metal ions with bovine brain phosphatidylserine vesicles by potentiometric and calorimetric titration methods. Two sizes of vesicle, 25 nm and 100 nm, were studied in 0.1 M NaCl at pH 7.4. The small vesicles were found to bind Ca^{2+} more strongly than the large vesicles. Ca^{2+} and Ba^{2+}, but not Sr^{2+} or Mg^{2+}, cause crystallization of the phospholipid acyl hydrocarbon chains with coincident destruction of the vesicles. Ca^{2+}-induced crystallization of the hydrocarbon chains occurs at approximately the same point on the Ca^{2+} binding isotherm at which charge neutralization of the vesicle surface occurs. Thermodynamic data for binding of Ca^{2+} and Mg^{2+} to small vesicles and for binding of Ca^{2+} to large vesicles are reported. Potentiometric titration data were used to obtain equilibrium constants for M^{2+} binding and the calorimetric titration data were used to obtain ΔH values. The potentiometric and calorimetric titration data are mutually supportive in establishing the stoichiometry and nature of the reactions occurring.

Introduction

Planar membranes, multilamellar liposomes, and both small and large bilayer vesicles of phospholipids serve as model systems for studying proposed mechanisms for divalent cation mediated cellular adhesion and fusion processes (for reviews see Refs. 1–3). The various models proposed for membrane fusion all involve either a phase change in the lipids of the membranes concerned [4,5] or crosslinking between bilayers [4,6] or some combination of both these mechanisms [5,7].

Phospholipid vesicles are also of interest as potential drug delivery vehicles. It may be possible to encapsulate drugs inside of vesicles, inject the vesicles, and obtain slow release or tissue specific release of the drugs (for review see Ref. 8.) For this reason it is necessary to more fully understand the stability of vesicles under physiological conditions and the mechanisms by which encapsulated materials may be released.

It has been well established, that for a specific pH and temperature, Ca^{2+} and Mg^{2+} can induce a disorder-to-order transition in bilayers of acidic phospholipids [9–14]. Portis et al. [6] showed that the addition of Ca^{2+} to small unilamellar phosphatidylserine (PS) vesicles at total Ca^{2+} concentrations of 1.3 and 5 mM at pH 7.4 and 25°C resulted in a rapid release of heat (−5.5 kcal/mol PS), but the addition of 5 mM Mg^{2+} or 0.7 mM Ca^{2+} produced only a small amount of heat (approx. 0.1 kcal/mol PS). It is not possible from

* Contribution No. 250 of the Thermochemical Institute.

0005-2736/82/0000–0000/$02.75

these measurements to relate the measured heat changes to the specific reaction steps occurring, but the large heat release apparently is the result of acyl chain ordering induced by Ca^{2+} [6].

Differential scanning calorimetry (DSC) studies of multilamellar PS liposomes prepared at pH 7.4 in 0.1 M NaCl have shown a single, very broad, asymmetric, thermally induced phase transition with the transition temperature being 11°C for Na^+-PS, 18°C for Mg^{2+}-PS and >100°C for Ca^{2+}-PS [6]. The enthalpy change for the transition was reported to be -4.5 ± 0.5 kcal/mol and to be associated with an acyl chain ordered-to-fluid phase transition. These data indicate that at physiological temperature the acyl chains in the Ca^{2+}-PS complex exist in an ordered state while the acyl chains in the Na^+-PS and Mg^{2+}-PS complexes exist in a fluid state.

Ca^{2+} coordination to phospholipids has been shown to be dependent upon pH and the concentrations of Na^+ and Mg^{2+} in a manner similar to coordination with long chain fatty acids [15]. Numerous studies using a wide variety of methodologies have been conducted on the binding of Ca^{2+} with PS. However, as pointed out in a recent study of Ca^{2+} interaction with PS by Holwerda et al. [16], there is poor agreement between the reported binding isotherms. This lack of agreement could be due to variations in pH [17], temperature, ionic strength, or vesicle size. Addition of Ca^{2+} to dilute small unilamellar PS bilayer vesicles has been shown to induce permeability of the vesicles to small ions and molecules at concentrations above approx. 0.5 mM Ca^{2+} [18]. The same study also showed that Ca^{2+} concentrations above 0.5 mM result in macroscopic aggregation, rupture, and formation of multilayer cylinders. No significant change in vesicle structure was observed upon the addition of Mg^{2+} until the Mg^{2+} concentration exceeded 5 mM. Above this concentration of Mg^{2+} the formation of multilayer liposomes was observed [18]. Similarly no increase in vesicle permeability is observed until the Mg^{2+} concentration exceeds 5 mM. Portis et al. [6] and Wilschut [19] reported the initiation of carboxyfluorescein release from small unilamellar PS vesicles at a Ca^{2+} concentration of 1 mM . Wilschut et al. [19] also found that initiation of carboxyfluorescein, Tb (citrate)$_3^{6-}$ and 2,6-pyridinedicarboxylic acid (sodium salt) release occurred at a Ca^{2+} concentration of approx. 1 mM for small unilamellar PS vesicles and at a Ca^{2+} concentration of approx. 2.5 mM for large unilamellar vesicles. Portis et al. [6] reported that aggregation as measured by light scattering occurred without release of sodium carboxyfluorescein from small bilayer vesicles at a mole ratio of Ca^{2+} bound to PS of approx. 0.4.

In this paper we report the results of calorimetric and potentiometric titrations of both large and small unilamellar PS vesicles with alkaline earth cations. The study was designed to provide thermodynamic data on Ca^{2+} binding to both sizes of vesicles at 25°C and pH 7.4. Mg^{2+} binding to small vesicles was also studied by both potentiometry and calorimetry. Only the calorimetric titrations could be done with Sr^{2+} and Ba^{2+} because suitable electrodes are not available for these cations.

Materials and Methods

Phosphatidylserine preparation

Phosphatidylserine, purified from bovine brain, was obtained from two sources. One sample was kindly supplied by Dr. D. Papahadjopoulos, Cancer Research Insitute, University of California at San Fransisco, CA, and the other was obtained from Avanti Biochemical, Birmingham, AL. These samples were stored as a chloroform solution in sealed glass ampules under argon at −40°C. A gas-liquid chromatographic examination of the methylated fatty acids prepared from these samples was in agreement with previously reported values [20]. The bovine PS is a mixture of 1,2-diacyl-*sn*-3-glycerophosphoserines. The acyl chain composition is 48% stearate (18:0), 36% oleate (18:1), and 16% longer unsaturated acyl chains. All other chemicals were purchased in the highest purity available. The water used was twice distilled from all-glass apparatus.

Vesicle preparation

Small unilamellar vesicles were prepared by a modification of the method described by Barenholz et al. [21]. The buffer system used in this study was 100 mM NaCl, 2 mM L-histidine and 2 mM *N*-tris(hydroxymethyl)methyl-2-aminoethanesulfonic acid (Tes) adjusted to a final pH of 7.4

with NaOH. The lipid was dried as a thin film under vacuum and dispersed in the above aqueous medium at a concentration of 10 mM and sonicated under argon at 20°C for 1 h in a bath-type sonicator. Large vesicles and/or aggregates were then removed from the preparations by centrifugation for 1 h at $115000 \times g$ in a Beckman SW 50.1 rotor. Usually more than 95% of the lipid was recovered in the supernate. Large unilamellar vesicles were prepared by the reverse phase evaporation technique previously described by Szoka and Papahadjopoulos [22], with modifications as described by Wilschut et al. [19]. The concentration of lipid was determined by measuring lipid phosphate as described by Bartlett [23]. The lipid preparation was adjusted to the desired concentrations by addition of buffer. All cation solutions were prepared in a NaCl, buffer solution identical to that used for the vesicles.

Differential scanning calorimetry (DSC)

The temperatures at which thermal transitions of the PS used in this study and of the alkaline earth metal-PS complexes precipitated from the buffer described above were determined using a prototype differential scanning calorimeter (DSC) manufactured by Hart Scientific, Provo, UT. Reliable ΔH values for the transitions were not obtained in this study because of calibration problems with the DSC.

Potentiometric titrations

The Ca^{2+} (neutral carrier), divalent-cation, and double junction reference electrodes were obtained from Orion Research Inc. (Cambridge, MA). The double junction, sleeved, reference electrode recommended by Orion Inc. for use with ion selective electrodes was employed for two reasons; (i) to prevent contamination of the sample with the electrolyte normally used in the reference electrode and (ii) to prevent clogging of the reference electrode during titrations of dispersions and precipitates [24]. The outer electrode filling solution, 0.1 M KNO_3, had the same ionic strength as the lipid dispersions. Results obtained at selected points using a flow system with the reference electrode located downstream from the Ca^{2+} electrode (Orion-SS20 electrode system) [25] were the same as the results from the titration experiments in which both electrodes were immersed in the same solution. The electrodes were used with a Radiometer PHM-64 research pH meter coupled to a recorder. The 0.1 M Ca^{2+} titrant solution was added with an automated buret in 1 to 2 μl increments to 5.0 ml of 2.0 mM PS. The 0.1 M Mg^{2+} titrant was added in 8 μl increments to 5.0 ml of 5.0 mM PS. Electrode potential readings in both cases were monitored until the value remained constant within a ± 0.2 mV region and then the next amount of titrant was added. This usually required waiting 2–3 min, the expected response time of the electrodes. The electrodes were not removed from the titrate solutions during the course of the titration. Calibration curves were obtained using standard Ca^{2+} or Mg^{2+} solutions in the same buffer solution as the lipid dispersions. Standard curves were measured before and after each lipid dispersion titration and were found to be reproducible to ± 1 mV. The sensitivity of the M^{2+} electrode was diminished at Mg^{2+} concentrations below 0.5 mM and as a result, measurements of Mg^{2+} below this concentration were less accurate. All potentiometric titrations were conducted at 25.0°C under an argon atmosphere.

Calorimetric titrations

Calorimetric titrations were performed in a Tronac isoperibol titration calorimeter at 25.0°C. Details of the 3 ml reaction vessel, data analysis and calculation procedures have been described [26–28]. In each case data points were taken automatically every 5 or 10 seconds. In all experiments at 25°C the 0.1 M M^{2+} titrant solution was added to 2.5 ml of 2.0 mM phospholipid solution. A 4.0 mM phospholipid solution was used in the experiments at 11°C. All solutions were prepared in the buffer solution described in the section on vesicle preparation. The heats of dilution of the titrant and PS solutions were determined by titrations of the buffer solution with 0.1 M M^{2+} in buffer and by titration of the vesicle dispersion with buffer solution, respectively. In most of the titrations, titrant was added continuously at 4.7 or 9.4 μl/min for 36 or 18 min, respectively. Some runs were also made with incremental addition of titrant to check for attainment of equilibrium, especially in those parts of the titration where large exothermic heat effects were observed.

Theory and calculations

The thermodynamic system of PS vesicles suspended in an aqueous solution must be treated as a multiphasic system. At least two phases are always present, i.e., the lipid and the aqueous phases, and more than two phases will be present if the lipid undergoes a phase change induced by metal ion binding. Since all of our work was done at approximately constant ionic strength, the activity coefficients in the aqueous phase will be approximately constant.

If the binding of M^{2+} to the surface of the bilayer is nonspecific or occurs at preexistent specific sites on the vesicle surface, then the binding isotherm may be described by the Langmuir isotherm (or the equivalent Scatchard model of independent, identical sites) or some modification thereof. Eqn. 1

$$\bar{n}/[M^{2+}] = NK - \bar{n}K \tag{1}$$

can be used to obtain the maximum number of divalent metal ions bound per PS molecule, N, and the intrinsic binding constant, K, from a plot of $\bar{n}/[M^{2+}]$ against $\bar{n}$ where $\bar{n}$ is the measured ratio of mol of M^{2+} bound to mol of PS and $[M^{2+}]$ is the measured molar concentration of M^{2+} in the aqueous phase [29].

If the binding of an M^{2+} ion causes a rearrangement of the lipid, i.e. a phase change, in the vesicles, then two possible situations arise depending on the miscibility of the new lipid phase with the previous lipid phase. When the two lipid phases are immiscible or nearly so, then the equilibrium concentration of M^{2+} must be constant. This can most easily be seen by writing the equilibrium constant expression for the reaction as shown in Eqn. 2 where a is the activity of the indicated species.

$$K = a(MPS_y)/a(PS_x)[M^{2+}] \tag{2}$$

Now, if the phases represented as MPS_y and PS_x are immiscible, the activities are invariant under isothermal and isobaric conditions and the equilibrium constant is equal to the inverse of $[M^{2+}]$ since the activities of the pure phases are unity by definition. In the other case when the two lipid phases are miscible, the activities of the two phases may be approximated by their mol fraction in the lipid phase. The Freundlich isotherm (or the equivalent Hill equation), Eqn. 3, is useful as a formalism for describing this latter kind of system. In Eqn. 3, θ is the mole fraction of lipid in the new phase with bound M^{2+}, K is the intrinsic binding constant for an divalent metal ion.

$$\theta/(1-\theta) = K^{\alpha}[M^{2+}]^{\alpha} \tag{3}$$

and α is the number of divalent metal ions which must be bound cooperatively in order to generate a domain of the new phase [29].

Thus, the appearance of a new immiscible lipid phase will be marked by the presence of a vertical region on a plot of $\bar{n}$ against $[M^{2+}]$, the presence of a new miscible lipid phase will be marked by a region of positive cooperativity of M^{2+} binding, i.e. $\alpha > 1$, and the binding of M^{2+} to preexisting sites on the vesicle surface will have $\alpha = 1$ or less.

Results

Potentiometric titrations

The data obtained in the potentiometric titrations are presented in Fig. 1. The data show that Ca^{2+} is bound more strongly to the small vesicles than to the large vescicles. Mg^{2+} is bound more strongly to the small vesicles than Ca^{2+} up to an $\bar{n}$ value of about 0.15 above which the Mg^{2+} is bound more weakly than CA^{2+}. The Mg^{2+} titration curve does not show the discontinuity at the initiation of precipitation which is seen in the Ca^{2+} titration curves of both the small and large vesicles at an $\bar{n}$ of approx. 0.2. However, precipitation begins at about the same $\bar{n}$ value in all three curves in fig.1. Note that the appearance of the Ca^{2+} precipitates is followed by a vertical region in Fig. 1 as expected when an immiscible new phase is being formed. Precipitation of both the small and large vesicles by Ca^{2+} is accompanied by a sudden uptake of Ca^{2+}, probably because of exposure of the previously inaccessible binding sites on the interior of the vesicle. After the precipitate is formed, Ca^{2+} continues to bind to the material formed from the small vesicles until $\bar{n}$ reaches nearly 0.6. Much less Ca^{2+} is bound by the precipitate from the large vesicles as shown by

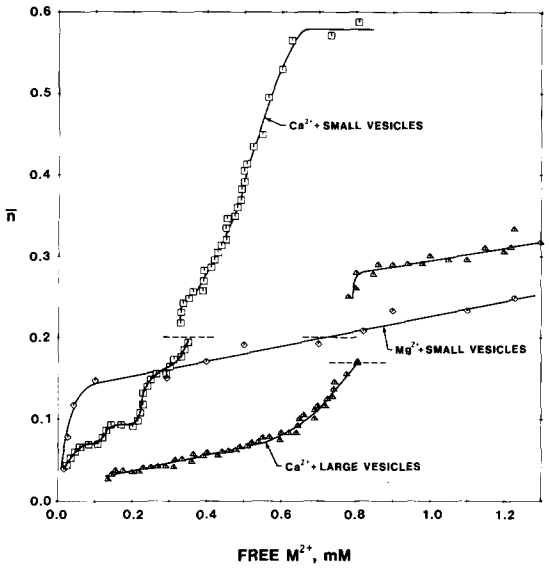

Fig. 1. Potentiometric titration curves for titration of small PS vesicles with Mg^{2+} and Ca^{2+} and of large PS vesicles with Ca^{2+} at 25°C in 0.1 M NaCl at pH 7.4. Experimental data points from a single titration are shown in each case. The dashed lines indicate the first appearance of turbidity.

the leveling off of the curve at an $\bar{n}$ value of 0.32.

The results of quantitative analysis as described above of the three curves given in Fig. 1 are given in Table I. In this analysis it is assumed that the interior of the vesicle is not available to the divalent ion until a critical metal ion concentration is reached. Other workers have previously found vesicles to begin to become permeable to small ions at a Ca^{2+} concentration near 0.5 mM and a Mg^{2+} concentration near 1 mM [18,30]. Prior to the point of permeability 60% of the PS is available for M^{2+} binding on the 25 nm vesicles and 50% on the 100 nm vesicles [31].

Mg^{2+} binding to small vesicles can be described within the limit of error of the measurements of unbound Mg^{2+} and up to the point of precipitation with a single intrinsic binding constant. The Mg^{2+} apparently binds to 3 PS molecules until the surface is saturated, i.e. $\bar{n}$ (surface) $= 0.33$ or $\bar{n} = 0.2$, at which point turbidity is first observed. The $\bar{n}$ value continues to increase beyond 0.2 in a linear manner with $[Mg^{2+}]$ and along the line shown in Fig. 1 at least up to $\bar{n} = 0.42$ and $[Mg^{2+}] = 3.5$ mM which is as far as data were taken. The turbidity also continues to increase throughout this part of the titration curve. These data are all consistent with the interior of the vesicles gradually becoming available for Mg^{2+} binding after the point of first appearance of the precipitate.

Two constants are required to describe the Ca^{2+} binding to the large vesicles. The first calcium ions are probably bound to 6 PS molecules (see Table I). After these PS_6 preexistent sites are populated, a cooperative rearrangement of the vesicle surface takes place resulting in one Ca^{2+} being bound to 3 PS molecules (i.e. $\bar{n}$ (surface) $= 0.3$). Precipitation occurs at $[Ca^{2+}] = 850$ μM. Very little further binding of Ca^{2+} occurs after precipitation is complete at an $\bar{n}$ of about 0.3.

The binding of Ca^{2+} to the small vesicles is the most complex situation. Ca^{2+} is first bound to a set of preexistent sites composed of 6 PS molecules per site until 70% of the lipid is complexed with Ca^{2+} (i.e. $0 < [Ca^{2+}] < 70$ μM. Secondly, Ca^{2+} is bound to a different set of sites, also composed of 6 PS molecules, but which must not have preexisted in the vesicle (i.e. 100 $\mu M < [Ca^{2+}] < 150$ μM). Binding of Ca^{2+} to this second set of sites is highly cooperative and involves several calcium ions simultaneously. Binding of Ca^{2+} to the third type of site begins at $[Ca^{2+}] \sim 200$ μM and continues until precipitation begins. These sites apparently consist of 3 PS molecules. Because of the invariance of the $[Ca^{2+}]$ at the midpoint of the sigmoid section of the curve at $[Ca^{2+}] = 229$ μM, the Gibbs phase rule requires that this new phase is not entirely miscible with the previously formed $Ca(PS)_6$ phase. Binding of Ca^{2+} to the $(PS)_3$ sites formed during this phase change continues until precipitation occurs. After precipitation is complete (at $\bar{n} = 0.25$), extensive further Ca^{2+} binding occurs, apparently accompanied by yet another phase change in the lipid.

Our results for binding constants are generally in agreement with previous data [16]. However, no previous study has obtained sufficient data to fully define the binding isotherms.

DSC measurements

In the DSC runs, single, broad, thermal transitions due to the melting of the acyl chains were observed for Na^+, Mg^{2+}, and Sr^{2+} salts of PS with transitions centered at 3–5°C, 18°C and 22°C,

TABLE I

PARAMETERS OF BINDING M^{2+} TO PS VESICLES AT pH 7.4 IN 0.1 M NaCl at 25°C

M^{2+} vesicles	K	PS/M^{2+} at binding site	Cooperativity parameters	Reaction
Mg^{2+}-small	$(1.8 \pm 0.4) \cdot 10^4$(a)	3.0 ± 0.2(a)		$Mg^{2+} + (PS)_3 = Mg(PS)_3$
Ca^{2+}-large	$(2.9 \pm 0.6) \cdot 10^3$(a)	6.6 ± 0.6(a)		$Ca^{2+} + (PS)_6 = Ca(PS)_6$
	$(1.6 \pm 0.1) \cdot 10^3$(b)	3(c)	8 ± 1 cooperative sites or 24 ± 3 PS molecules(b)	$Ca^{2+} + Ca(PS)_6 = 2Ca(PS)_3$
	$(1.2 \pm 0.1) \cdot 10^3$(d)	3(c)	precipitation	$Ca(PS)_3(1) = Ca(PS)_3$(cryst.)
Ca^{2+}-small	$(3.1 \pm 0.2) \cdot 10^4$(a)	6.0 ± 0.1(a)		$Ca^{2+} + (PS)_6 = Ca(PS)_6$
	$(8.1 \pm 0.5) \cdot 10^3$(e)	6(c)	24 ± 6 cooperative sites or 144 ± 36 PS molecules(e)	$Ca^{2+} + 6\ PS = Ca(PS)_6$
	$(4.4 \pm 0.1) \cdot 10^3$(d)	3(c)	phase transition in vesicle	$Ca(PS)_6 = Ca(PS)_3 + (PS)_3$
	$(4.8 \pm 0.2) \cdot 10^3$(b)	3(c)	4.7 ± 0.6 cooperative sites or probably 2 $Ca(PS)_6$ complexes(b)	$CA^{2+} + (PS)_3 = Ca(PS)_3$
	$(2.9 \pm 0.1) \cdot 10^3$(d)	4(c)	precipitation	$Ca(PS)_3 + PS(interior) = Ca(PS)_4$(cryst.)
	$(2.6 \pm 0.1) \cdot 10^3$(f)	2(c)	4.5 ± 0.3 cooperative sites or 9 ± 0.6	$Ca^{2+} + Ca(PS)_4$(cryst.) $= 2Ca(PS)_2$(cryst.)

(a) From a plot of $\bar{n}$(surface)/$[M^{2+}]$ versus $\bar{n}$(surface).
(b) From a Hill plot assuming saturation at $\bar{n} = 0.333$.
(c) As indicated by a horizontal region or other feature in the $\bar{n}$ versus $[M^{2+}]$ curve, Fig. 1.
(d) K equals the reciprocal of the $[M^{2+}]$ as explained in the calculation section.
(e) From a Hill plot assuming saturation at $\bar{n} = 0.167$.
(f) From a Hill plot assuming saturation at $\bar{n} = 0.500$.

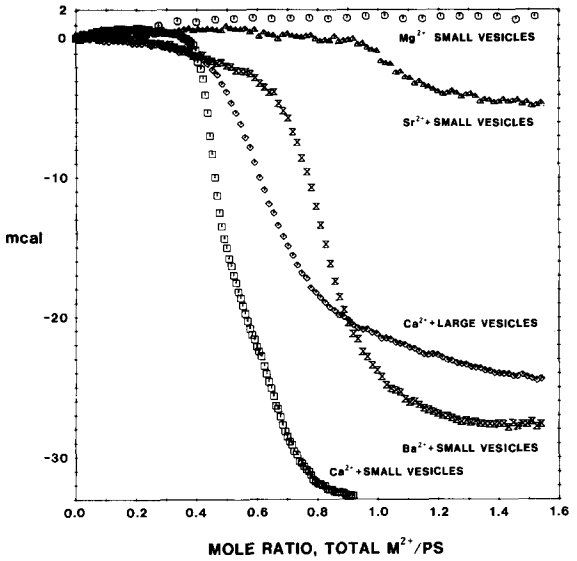

Fig. 2. Calorimetric titration curves for titration of small PS vesicles with Mg^{2+}, Sr^{2+}, Ba^{2+}, and Ca^{2+} of large PS vesicles with Ca^{2+} at 25°C in 0.1 M NaCl at pH 7.4.

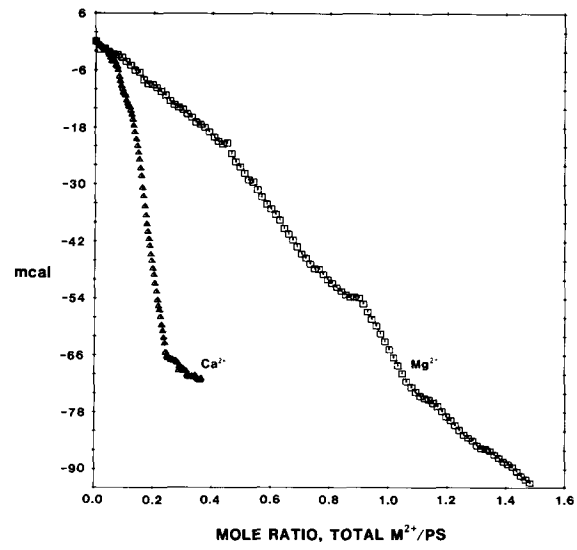

Fig. 3. Calorimetric titration curves for titration of small PS vesicles with Mg^{2+} and Ca^{2+} at 11°C in 0.1 M NaCl at pH 7.4.

respectively. The transitions were 2–3°C wide at half the peak height. The transition temperatures obtained for the Na^+ and Mg^{2+} salts are in agreement with previous DSC values [12] and laser Raman spectral measurements [14]. The transitions temperatures for both the Ca^{2+} and Ba^{2+} salts are above 90°C. The ΔH values for the thermal transitions of the Na^+, Mg^{2+}, and Sr^{2+} salts are approximately equal.

Calorimetric titrations

In Fig. 2 are shown the calorimetric titration curves for the continuous titration of the small unilamellar vesicles with Mg^{2+}, Ca^{2+}, Sr^{2+} and Ba^{2+} and of the large unilamellar vesicles with Ca^{2+}. In all cases the heat effects are small for the reaction(s) which occur up to a mol ratio of total metal ion to PS of about 0.35. These small heat effects are consistent with complexation of Ca^{2+} with either carboxylate or phosphate ligands [32]. Heat effects continue to be relatively small throughout the titrations with Mg^{2+} and Sr^{2+}. A reaction(s) having a large exothermic ΔH value(s) begins at an M^{2+}/PS ratio of about 0.35 in the binding of Ca^{2+} with both large and small vesicles and at a somewhat larger ratio in the binding of Ba^{2+} to the small vesicles. The beginning of the exothermic reaction coincides with the onset of precipitation as indicated on the potentiometric titration curves shown in Fig. 1. Because, as shown by the DSC data, the acyl chains are crystallized in the Ca^{2+} and Ba^{2+} salts but not in the Mg^{2+} and

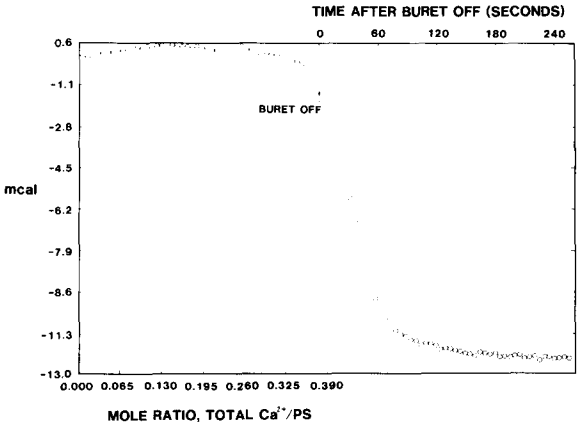

Fig. 4. Incremental calorimetric titration of small PS vesicles with Ca^{2+} at 25°C in 0.1 M NaCl at pH 7.4.

TABLE II

RESULTS OF INCREMENTAL CALORIMETRIC TITRATION OF SMALL UNILAMELLAR VESICLES WITH Ca^{2+} AT 25°C IN 0.1 M NaCl AT pH 7.4

Addition	Total Ca^{2+} / Total PS	$\bar{n}$	Incremental Q(mcal)	Total Q(mcal)
1	0.202	0.096	−0.08	−0.08
2	0.376	0.212	−17.2	−17.3
3	0.532	0.313	−8.6	−25.9
4	0.843	0.530	−2.9	−28.8

Sr^{2+} salts of PS at 25°C, we reason that titration of PS vesicles at 25°C with Mg^{2+} or Sr^{2+} will not induce a transition to the crystalline state, but addition of sufficient Ca^{2+} or Ba^{2+} will induce crystallization of the PS acyl chains. Thus, the large exothermic heat effect must be caused by crystallization of the acyl chains in the PS. The small exotherm in the Sr^{2+} titration curve is probably due to partial crystallization of the PS since the transition temperature of this salt is centered only 3 K below 25°C. Further evidence that the large exothermic effect is caused by acyl chain crystallization is the agreement of the heat obtained during the precipitation of small vesicles with Ca^{2+}, -4.9 ± 0.7 kcal/mol of lipid, with the negative of the heat of melting of the lipid in a multilamellar state as determined by DSC measurements, -4.5 ± 0.5 kcal/mol [6]. The value of ΔH obtained in this study for the overall reaction of Ca^{2+} with small vesicles, -5.6 ± 0.7 kcal/mol of lipid, is also in agreement with the value, −5.5 kcal/mol of lipid, determined by batch calorimetry by Portis et al. [6].

If crystallization of the acyl hydrocarbon chains is the cause of the large exothermic effect seen in Fig. 2 for Ca^{2+} and Ba^{2+} at 25°C, then calorimetric titrations with Mg^{2+} at a temperature below 18°C should show a similar large exothermic ef-

TABLE III

THERMODYNAMICS OF M^{2+} BINDING TO PS IN 0.1 M NaCl AT pH 7.4

Values are at 25°C unless noted otherwise.

Reaction	$\Delta G°$ (kcal/mol)	$\Delta H°$ (kcal/mol)	$\Delta S°$ (cal/mol/K)
Mg^{2+}-small vesicles			
$Mg^{2+} + (PS)_3\text{-}Mg(PS)_3$	-5.8 ± 0.1	1.4 ± 0.4	24 ± 1
Mg^{2+} + small vesicles = final product [a]	–	(>8.0)(11°C) [c]	–
Ca^{2+}-large vesicles			
$Ca^{2+} + (PS)_6 = Ca(PS)_6$	-4.7 ± 0.1	$+1.9 \pm 0.7$	22 ± 2
$Ca^{2+} + Ca(PS)_6 = 2Ca(PS)_3$	-4.37 ± 0.04	-1.7 ± 1.1	9 ± 4
$Ca(PS)_3(1) = Ca(PS)_3$(cryst.)	-4.20 ± 0.05	-1.29 ± 1.2	-29 ± 4
		(-4.3 ± 0.4) [c]	
Ca^{2+}-small vesicles			
$Ca^{2+} + (PS)_6 = Ca(PS)_6$	-6.12 ± 0.04	$+1.2 \pm 0.3$	25 ± 1
$Ca^{2+} + 6PS = Ca(PS)_6$	-5.3 ± 0.03	-0.4 ± 1.0	17 ± 3
$Ca(PS)_6 = Ca(PS)_3 + (PS)_3$	-4.97 ± 0.02	0.0 ± 2.0	17 ± 6
$Ca^{2+} + (PS)_3 = Ca(PS)_3$	-5.02 ± 0.03	-1.0 ± 0.2	13 ± 1
$Ca(PS)_3 + PS(int.) = Ca(PS)_4$(cryst.)	-4.72 ± 0.02	-19.6 ± 2.8	-50 ± 9
		(-4.9 ± 0.7)	
$Ca^{2+} + Ca(PS)_4$(cryst.) $= 2\ Ca(PS)_2$(cryst.)	-4.66 ± 0.03	-2.7 ± 0.5	7 ± 2
Ca^{2+} + small vesicles = final product [a]	–	(-6.9 ± 1.0) (11°C) [c]	–
Ba^{2+}-small vesicles			
Ba^{2+} + small vesicles = final product [b]	–	(-4.1 ± 0.4) [c]	–

[a] See Fig. 3.
[b] See Fig. 2.
[c] kcal/mol lipid.

fect. Fig. 3 shows thermograms for the titration of small vesicles with Mg^{2+} and Ca^{2+} at 11°C. As predicted, the Mg^{2+} titration shows a large exothermic effect consistent with that expected for acyl chain crystallization although the shape of the curve is different from the Ca^{2+} titration thermogram. The Ca^{2+} titration thermogram is not significantly altered by the temperature change from 25°C.

The highly exothermic reactions observed with Ca^{2+} and Ba^{2+} at 25°C are slow compared to the continuous titration rate, and thus, the shape of this portion of the thermograms shown in Fig. 2 is determined by the kinetics of the reactions and not by the amount of titrant added. The thermogram shown in Fig. 4 illustrates this fact. In order to obtain ΔH values for the reactions occurring during and after precipitation, an incremental titration of the small vesicles with Ca^{2+} was made in the calorimeter. The results form the incremental addition of Ca^{2+} are given in Table II. These data show that the binding of Ca^{2+} to PS is accompanied by small heat effects both before and after precipitation of the PS. Thus, since crystallization of the acyl chains is the only process occurring in this system with a large heat effect, crystallization of the acyl chains coincides with the Ca^{2+} precipitation reaction. The ΔH values calculated from the calorimetric titration data are given in Table III together with other derived thermodynamic quantities.

An experiment designed to show that removal of Ca^{2+} from the Ca^{2+}-PS complex would result in disordering of the acyl chains was conducted in the following manner. First, a calorimetric titration of PS with 0.1 M Ca^{2+} was conducted until the ratio of total Ca^{2+} to PS was 1.0. Without removing the tiration vessel the resultant Ca^{2+}-PS complex was then titrated with 0.1 M EDTA. After making the appropriate corrections for the heat of the EDTA reaction with Ca^{2+} as obtained in a separate titration, we found an endothermic heat associated with the order-to-fluid transition of 5.0 $\pm$ 1.0 kcal/mol of PS. The vesicles formed during titration with EDTA will be much larger than the initial vesicle size and will also be multilayer [33]. This experiment shows that crystallization of the acyl chains is indeed induced by Ca^{2+} and that removal of Ca^{2+} reverses the process.

Discussion

The results of the potentiometric and calorimetric titrations done in this study are mutually supportive in that all of the end points found in one type of data were also present in the other type. The end-points are often more easily and accurately found in one type of data than in the other, but in no case were the potentiometric and calorimetric data in disagreement.

A complete description of M^{2+} binding to PS vesicles must take into account the binding of monovalent cations, i.e. Na^+ and H^+ in the solutions used in this study. We assume that these monovalent cations are bound competitively with M^{2+} in the reactions in Table III. However, both Na^+ and H^+ were held constant in this study so no effect could be observed.

The greater strength of binding of Ca^{2+} to small vesicles as compared to large vesicles prior to precipitation is probably the result of two factors: (i) the smaller radius of curvature in small vesicles results in greater separation of the exterior phosphoserine groups and (ii) the heterogeneity of the acyl chains could result in greater staggering of the serine moieties in the small vesicles [34]. Dawson and Hauser [15] reported that the interaction of Ca^{2+} with PS monolayers increased with an increase in the area occupied per PS molecule. This observation is in agreement with our comparison of small and large vesicles. The greater complexity of the Ca^{2+} binding to the small vesicles is probably a result of the same two factors. We cannot evaluate the importance of the heterogeneity of the PS until further are done on pure phospholipid systems.

The potentiometric titration curves of both small and large vesicles with Ca^{2+}, Fig. 1, have a discontinuity at the same point at which the large exotherm begins in the calorimetric titration curves, Fig. 2. As explained in the Results, the large exotherm is caused by crystallization of the acyl chains. The discontinuity is the potentiometric curves is caused by a sudden uptake of Ca^{2+} by the PS. Turbidity is also first observed in the solutions at this point. The concentration of free Ca^{2+} is the aqueous phase remains constant on addition of further small amounts of Ca^{2+}. All of these observations are consistent with the ap-

pearance of a crystallized lipid phase and a concomitant distruction of vesicle integrity. The sudden uptake of Ca^{2+} can be explained by the availability of PS binding sites which were previously on the inaccessible interior of the vesicle. Several other workers have reported significant effects to occur at the same $\bar{n}$ value, i.e. 0.36 Ca^{2+}/surface PS, at which we observe the discontinuity and the beginning of the exotherm [6,19,30]. We have chosen to refer to the exothermic process which begins at the discontinuity as precipitation in order to avoid confusion with several other terms, i.e. coalescence, aggregation, and fusion, which have been used to describe what we believe is the same phenomenon. Also, precipitation is a well defined word meaning the separation of an immiscible or insoluble phase from a solution or suspension and implies nothing about the structure of the precipitate. The structures of Ca^{2+} and Mg^2-PS obtained under conditions similar to those used in this study have been shown to vary greatly from each other and with small changes in the precipitation conditions [18]. Also included in the observations of others is that PS vesicles are approximately charge neutralized and begin to leak small ions at about 0.3 divalent metal ions/surface PS [18,30]. Large molecules and polyatomic ions are apparently not lost until crystallization of the acyl chains is nearly complete [6,19]. The structure of the precipitate is thus of importance and further investigation of the structure of the precipitates is necessary to resolve the mechanism(s) involved in release of encapsulated materials. It is of interest to note here that the free Ca^{2+} concentration (ionized) is blood plasma and interstitial fluid ranges between 0.8 and 1.2 mM, and thus the small vesicles would be precipitated whereas the large vesicles should retain their encapsulated contents.

The fact that all the coordination site(s) of small vesicles become available after precipitation by Ca^{2+} but not in the case of large vesicles suggests that the structure of the precipitates is a function of vesicle size. The potentiometric titration data suggest that the product of precipitation of the small vesicles has the overall formula $Ca(PS)_4$ while that from the large vesicles is $Ca(PS)_4$ (see Fig. 1). The precipitate from the large vesicles is obviously less stable than the $Ca(PS)_4$ or $Ca(PS)_2$ phases from the small vesicles, but no conversion apparently takes place, and therefore there must not be a low energy for conversion of one precipitate to the other. This result may explain the variety of particle shapes and sizes which have been observed in Ca-PS precipitates obtained under varying conditions [18]. The fact that less heat is obtained during the precipitation of large vesicles with Ca^{2+} than during precipitation of small vesicles (see Fig. 2) suggests that acyl chain crystallization is incomplete in the large vesicle precipitate and thus that part of the PS is not bound to Ca^{2+}. The crystallized part of the PS probably has the same Ca^{2+} to PS ratio as the small vesicle precipitate, i.e. $Ca(PS)_2$.

In the titration of small vesicles with Mg^{2+}, turbidity appears at the same ratio of bound Mg^{2+} to surface lipid, i.e. 0.36. However, no discontinuity is seen in the potentiometric titration curve and no exotherm is seen in the calorimetric titration at 25°C. These results are consistent with previously reported freeze-fracture electron micrography studies which indicate no significant macroscopic changes in vesicle structure can be seen upon addition of Mg^{2+} until the Mg^{2+} concentration exceeds 5 mM [18]. However, loss of small ions from the vesicles begins to occur at 1 mM Mg^{2+} [30]. It is evident that the structural changes induced by Ca^{2+} at the point of precipitation are not solely a result of vesicle surface charge neutralization, as charge neutralization due to Mg^{2+} is the same at the same $\bar{n}$ value, but the structural collapse of the vesicle does not occur with Mg^{2+}. The structural collapse caused by Ca^{2+} must be associated with acyl chain ordering. The calorimetric data given in Fig. 1 therefore show that Ba^{2+} will also induce vesicle rupture, but Sr^{2+} will not at 25°C.

The alternating order in the alkaline earth ion effectiveness at causing acyl chain crystallization is remarkable is view of the regular trends in periodic properties which exist in this group of ions. The alternating sequence may be due to a difference in the binding to the phosphoserine (e.g. carboxylate vs. phosphate or intra- vs. inter-molecular chelation, etc.) and/or to a difference in the state of hydration of the complexed metal ion. All attempts to determine the metal ion binding site have been inconclusive or contradictory. Infrared

studies give evidence for carboxylate involvement in Ca^{2+} binding [16] while NMR results implicate the phosphate group as the Ca^{2+} binding site [2]. Thus the M^{2+} coordination site(s) of phosphatidylserine remains an unresolved issue [2,16]. The results of the infrared and NMR studies do show, however, that binding of M^{2+} leads to a tighter packing of the phosphoserine groups [2,16]. It is this effect which probably caused acyl chain crystallization and vesicle disruption. The state of hydration of the bound cations is also not known. Literature data on cation hydration in alkaline earth salts of fatty acids do suggest that the Mg^{2+} and Ca^{2+} salts of PS are probably hydrated while the Ba^{2+} salt is not [35–37]. This could explain the anomalous position of Sr^{2+} in our results.

Conclusions

The most important conclusion to be drawn from this work is that the properties of unilamellar phospholipid vesicles are a strong function of the vesicle size. The binding constants for Ca^{2+} binding to 25 nm PS vesicles are considerably larger than those for 100 nm PS vesicles. Also, the complexity of the binding reactions with Ca^{2+} is much greater for small vesicles than for large ones. The precipitates produced by reaction of Ca^{2+} with small and large vesicles are also different in both composition and further reactivity towards Ca^{2+}. Ca^{2+} cause crystallization of the phospholipid acyl chains coincident with the precipitation reaction. Mg^{2+} and Sr^{2+} cause precipitation but not acyl chain crystallization unless the temperature is below 18 or 22°C, respectively. We believe the precipitation reaction to be the same phenomenon which has been variously referred to as coalescence, fusion, and aggregation by others. The acyl chain crystallization is the same process which is thermally induced in DSC experiments with metal salts of PS.

Acknowledgements

This work was supported in part by the Veterans Research Service, Veterans Administration Medical Center, San Francisco, CA. We also would like to thank Dr. N. Duzgunes (Cancer Research Institute, San Francisco, CA) for aid in preparing some of the vesicle dispersions used in our experiments and Dr. W.J. Leonard, Jr. (Research Section, Winthrob Insurance Inc., San Francisco, CA) for valuable discussions concerning drug delivery systems.

References

1 Melchior, D.L. and Steim, J.M. (1976) Annu. Rev. Biophys. Bioeng 5, 205–238
2 Hauser, H. and Phillips, M.C. (1979) Prog. Surface Membrane Sci. 13, 197–412
3 Gratzl. M., Schudt, C., Ekerdt, R. and Dahl, G. (1980) in Membrane Structure and Function (Bittar, E.E., ed.), Vol. 3, pp. 59–52, Wiley, New York
4 Lucy, J.A. (1970) Nature 227, 815–817
5 Ohnishi, S. and Ito, T. (1974) Biochemistry 13, 881–887
6 Portis, A., Newton, C., Pangborn, W. and Papahadjopoulos, D. (1979) Biochemistry 18, 780–790
7 Hui, S.W., Stewart, T.P., Boni, L.T. and Yeagle, P.L. (1981) Science 212, 921–922
8 Juliano, R.L. and Layton, D. (1980) in Drug Delivery Systems (Juliano, R.L., ed.), pp. 189–236, Oxford University Press, Oxford
9 Trauble, H. and Eibl, H. (1974) Proc. Natl. Acad. Sci. U.S.A. 71, 214–219
10 Verkleij, A.J., De Kruijff, B., Ververgaert, P.H.J.T., Tocanne, J.F. and Van Deenen, L.L.M. (1974) Biochim Biophys. Acta 339, 432–437
11 Van Dijck, P.W.M., Ververgaert, P.H.J.T., Verkleij, A.J., Van Deenen, L.L.M. and De Gier, J. (1975) Biochim Biophys. Acta 406, 465–478
12 Jacobson, K. and Papahadjopoulos, D. (1975) Biochemistry 14, 152–161
13 MacDonald, R.C., Simon, S.A. and Baer, E. (1976) Biochemistry 15, 885–891
14 Hark, S.K. and Ho, J.T. (1979) Biochem. Res. Commun. 91, 665–670
15 Dawson, R.M.C. and Hauser, H. (1970) in Calcium and Cellular Function (Cuthhert, A.W., ed.), pp. 17–41, MacMillan, New York
16 Holwerda, D.L., Ellis, P.D. and Wuthier, R.E. (1981) Biochemistry 20, 418–428
17 Abramson, M., Katzman, R. and Greger, H.P. (1964) J. Biol. Chem. 239, 70–76
18 Papahadjopoulos, D., Vail, W.J., Newton, C., Nir, S., Jacobson, K., Poste, G. and Lazo, R. (1977) Biochim. Biophys. Acta 465, 579–598
19 Wilschut, J., Duzgunes, N., Fraley, R. and Papahadjopoulos, D. (1980) Biochemistry 19, 6011–6021
20 Hauser, H. and Phillips, M.C. (1973) J. Biol. Chem. 248, 8585–8591
21 Barenholz, Y., Gibbs, D., Litman, B.J., Goll, J., Thompson, T.E., and Carlson, F.D. (1977) Biochemistry 16, 2806–2810
22 Szoka, F., Jr. and Papahadjopoulos, D. (1978) Proc. Natl. Acad. Sci. U.S.A. 75, 4194–4198
23 Bartlett, G.R. (1959) J. Biol. Chem. 234, 466–468

24 Cammann, K. (1979) Working with Ion Selective Electrodes, pp. 41–42, Springer-Verlag, New York
25 Rehfeld, S.J., Duzgunes, N., Newton, C., Papahadjopoulos, D. and Eatough, D.J. (1981) FEBS Lett. 123, 249–251
26 Hansen, L.D., Jensen, T.E., Mayne, S., Eatough, D.J., Izatt, R.M. and Cristensen, J.J. (1975) J. Chem. Thermodyn. 7, 919–926
27 Hansen, L.D., Izatt, R.M., Eatough D.J., Jensen T.E. and Christensen, J.J. (1975) Analytical Calorimetry, Vol. 3, 7–16 (Porter, R.S. and Johson J.F., eds.), Plenum Press, New York
28 Eatough, D.J., Rehfeld, S.J., Izatt, R.M. and Christensen, J.J. (1982) in Biochemical and Clinical Applications of Thermal and Thermometric Analysis (Jespersen, N., ed.), Chap. 7, Elsevier, Amsterdam
29 Cantor, C.R. and Schimmel, P.R. (1980) Biophysical Chemistry, Part III, pp. 852–866, W.H. Freeman, San Francisco
30 Papahadjoulos, D. and Ohki, S. (1970) in Liquid Crystals and Ordered Fluids (Johnson, J.F. and Porter, R.S., eds.), pp. 13–32, Plenum Press, New York
31 Huang, C. and Mason, J.T. (1978) Proc. Natl. Acad. Sci. U.S.A. 75, 308–310
32 Christensen, J.J., Eatough, D.J. and Izatt, R.M. (1975) Handbook of Metal Ligand Heats, Marcel Dekker, New York
33 Sun, S.-T., Day, E.P. and Ho, J.T. (1978) Proc. Natl. Acad. Sci. U.S.A. 75, 4325–4328
34 Barton, P.G. (1968) J. Biol. Chem. 243, 3884–3890
35 Hoppler, F. (1942) Fette Seifen 49, 700–708
36 Vold, R.D., Grandine, J.D. and Vold, M.J. (1948) J. Colloid Sci. 3, 339–361
37 Lesslauder, W. and Blasie, J.K. (1972) Biophys. J. 12, 175–190